ECCE AB 21

virtual event

Engineering the Future

13th European Congress on Chemical Engineering
6th European Congress on Applied Biotechnology
20-23 September 2021

The meeting point for researchers across Europe and the world with

- 13 parallel sessions
- Science Slam
- ChemCar Competition
- Virtual exhibition

Find out more and register at ecce-ecab2021.eu

Plenary speakers

Jiří Drahoš,
Senator of the Czech
Parliament Prague/CR

Michael Doherty
University of California
Santa Barbara CA/USA

Luisa Freitas Dos Santos
GlaxoSmithKline plc.
Brentford/UK

Melanie Maas-Brunner
BASF SE
Ludwigshafen/D

Emily Nguyen
Palantir Technologies
New York/USA

Platinum Sponsor

BASF
We create chemistry

Silver Sponsors

Research and Development

Beiersdorf

Organizer

DECHEMA

Supporter

EFCE

ESBES

Batch Oxidative Desulfurization of Model Light Gasoil Over Bimetallic Nanocatalyst

Layth T. Abdulateef[1], Amer T. Nawaf[2], Prof. Dr. Omer Yasin Thayee Al-Janabi[2]*, Prof. Dr. Peter J. S. Foot[3], Qahtan A. Mahmood[2]
[1]Middle Technical University, Department of Chemical Engineering, PO.B., 10001 Baghdad, Iraq
[2]Tikrit University, Department of Petroleum & Gas Refining Engineering, PO.B., 34001 Tikrit, Iraq
[3]Kingston University, Department of Chemistry and Pharmaceutical Sciences, KT1 2EE Kingston upon Thames, UK
*Correspondence: Prof. Dr. Omer Yasin Thayee Al-Janabi (E-mail: omaroilgas@tu.edu.iq), Tikrit University, Department of Petroleum & Gas Refining Engineering, PO.B., 34001 Tikrit, Iraq

Abstract

This work explored the design and synthesis of a novel AgO/ZnO/HY-Zeolite bimetallic nanocatalyst by an impregnation method. The purpose of this nanocatalyst was to remove the dibenzothiophene as the primary sulfur content from a light gasoil model via a catalytic oxidative desulfurization process (ODS). The characteristics of the synthesized nanocatalyst were determined by FTIR, BET, SEM, and XRD. The synthesized nanocatalyst indicated an area of 252 m^2g^{-1}, pore volume and pore size equal to 0.221 cm^3g^{-1} and 2.15 A^o, respectively. The ODS results revealed better sulfur conversion i.e. 91.8% conversion efficiency at optimal ODS reaction conditions. The results also indicated very good reusability of the synthesized catalyst after recycling five times.
Keywords: HY-Zeolite, Oxidative desulfurization (ODS), Sliver oxide (AgO), Zinc Oxide (ZnO)

1 Introduction

Organic sulfur compounds like thiophenes (Th), benzothiophenes (BT), dibenzothiophenes (DBT) and their alkyl derivatives (see S1 in supporting information) are the major undesired species present in crude oil. These compounds, however, are the foremost pollutants exporters that contribute to the release of SO_x and acid rain to the environment [1-5]. In addition, organic sulfur has a negative impact on the performance of automotive engine exhaust inhibitors as it irreversibly poisons noble metal catalysts in the converter. Furthermore, organic sulfur in diesel fuel causes serious corrosion in transportation pipelines and deactivation of the catalyst used in the downstream processes as well as reducing combustion efficiency and increasing emission of particulates [6-10]. For the above-mentioned reasons, thorough desulfurization of diesel fuel is attracting more and more attention worldwide to produce green diesel meet the stringent global environmental regulations on transportation fuels [11-18]. In petroleum refineries, the removal of organic sulfur from petroleum distillates such as diesel fuel is mainly achieved via conventional hydrodesulfurization (HDS). However, due to its severe operating conditions in terms of high reaction temperature and pressure,

Received: February 09, 2021; revised: June 19, 2021; accepted: July 16, 2021

To be cited as: Chem. Eng. Technol. 10.1002/ceat.202100027

Link to final VoR: https://doi.org/10.1002/ceat.202100027

HDS has significantly elevated operating costs and is less effective in eliminating refractory sulfur compounds; hence it may not be the optimum desulfurization process [19, 20]. Recently, sophisticated technologies such as catalytic oxidative desulfurization (Cat-ODS), selective adsorption, bio-desulfurization and oxidation-extraction have been used for the production of ultra-low sulfur fuels [21-23]. Catalytic oxidative desulfurization (Cat-ODS), on the other hand, has proven to be one of the most potent recent alternatives to HDS [24, 25]. In the ODS process, an oxidant such as hydrogen peroxide, organic peroxide, air and/or molecular oxygen is typically used to oxidize the alkyl-substituted sulfur compounds in diesel fuel to their sulfones and sulfoxides counterparts. These oxidized species are then extracted from the ODS product stream by a suitable solvent, and any remaining oxidant is removed by water [26]. In the ODS process, air is preferred over other oxidizing agents owing to its safety, availability, lack of side-reactions and ecofriendliness [27]. However, choice of a suitable catalyst for the oxidative desulfurization process is regarded as a crucial factor for selectivity and sulfur removal efficiency. High oxidation state transition metals on various inorganic supports like alumina and zeolites are the predominant active catalysts for Cat-ODS [15, 28-30]. Furthermore, hybrid inorganic nanocomposites could also be a novel strategy for developing multifunctional nanocatalyst with catalytic and adsorptive capabilities that are ideal for ODS process [31-35]. This contribution, however, is focused on batch oxidative desulfurization of model light gasoil over newly designed hybrid inorganic nanocomposite catalyst. Among nano-supports, HY zeolite nanoparticles are a promising adsorptive support for certain metal oxide catalysts. Therefore, commercially available HY zeolite nanoparticles were decorated with silver and zinc oxides by an impregnation method to synthesize a novel hybrid bimetallic nanocatalyst for removing organic sulfur from a model light gasoil. The selection of zinc and silver oxides as active components for our new designed nanocatalyst was based on the superior catalytic activity of zinc oxide and the high selectivity of silver oxide towards sulfur compounds. The physical properties of the synthesized nanocatalyst were determined by Fourier-Transform IR Spectroscopy, Brunauer-Emmett-Teller (BET) analysis, Scanning Electron Microscopy (SEM) and X-Ray Diffractometry. Oxidative desulfurization operating variables were optimized for high ODS efficiency using a batch three-necked reactor vessel.

2 Materials and Method

2.1 Materials

All chemicals and reagents utilized in the catalyst preparation were of analytical grade with 99% purity and were used as-received. Deionized water used in the synthesis of nanocatalyst was Milli-Q water (resistivity greater than 18.2 MΩ.cm), supplied by Al-Doora Refineries Iraq. Air as an oxidizing agent was supplied by a compressor in College of Petroleum Process Engineering Tikrit University. Organic sulfur (DBT) M.Fw: $C_{12}H_8S$, M.wt:184.26°C, silver nitrate ($AgNO_3$), zinc acetate [$Zn(CH_3CO_2)_2{\cdot}2H_2O$], and commercial HY-zeolite with (80~100 mesh) were all purchased from Sigma Aldrich UK. Model Light gasoil having the physical properties illustrated in Table 1 was supplied from the Ministry of Oil Iraq.

2.2 Instrumentation

FTIR spectra of the synthesized nanocatalyst (as pellets in KBr) were recorded with an IR Shimadzu 8400 spectrophotometer over the range of 400-4000 cm^{-1}. The crystalline structures of the synthesized nanocatalyst was characterized by XRD using a Rigaku Miniflex diffractometer with Cu Kα source (λ= 1.5406Å). N_2 adsorption-desorption isotherms of the pristine HY-zeolite and AgO/ZnO/HY-zeolite nanocatalyst were performed to measure the specific surface areas of the samples, according to the Brunauer-Emmett-Teller (BET) method, and pore volumes with the Barret-Joyner-Halenda (BJH) model. The surface morphology of the obtained nanocomposite was examined by scanning electron microscopy (SEM) (Model: ZEISS Sigma 300). Sulfur content after each run of Cat-ODS was

measured by XOS Sindie 7039 XRF Trace Sulfur Fast Batch Testing Fuel Analyzer at the Petroleum Research Centre Ministry of Oil Iraq.

Table1: Physical properties of the model light gasoil (LGO)

Model Light Gasoil (LGO)			
API gravity	37.2	Distillation	Temp °C
Viscosity, sct at 293K	4.8	Initial boiling point IB	157
Flash point °C	56	10%	198
Cetane index	51	50%	261
Specific gravity	0.873	90%	345
DBT content, ppm	1200	End boiling point EP	355

2.3 Design and synthesis of AgO/ZnO/HY-zeolite bimetallic nanocomposite catalyst

The design and synthesis steps of the bimetallic nanocomposite catalyst are described in the supporting information.

2.4 Batch oxidative desulfurization experimental design

The details for the ODS experimental design are included in supporting information.

3 Results and discussion

3.1 FTIR analysis

FTIR (400-4000 cm^{-1}) was used to probe the surface chemistry and acidity of the synthesized nanocatalyst. Samples were prepared by mixing 1:99 wt% of the nanocatalyst to KBr powder and pressed into disks. The characteristic peaks of the nanocomposite catalyst are presented in (Fig. 1). The faujasite structure of HY-zeolite featured stretching bands at 3462-3491 cm^{-1} corresponding to the Brønsted acid protons in the sodalite cage, SiO_4 molecules and Al-OH linkages. Distinctive bands around 800-810 cm^{-1}, 1015-1026 cm^{-1} and 1150 cm^{-1} were respectively correlated to the symmetric stretching, internal and external tetrahedral asymmetrical stretching vibration bands of SiO_4 or AlO_4 units. The bands at 1015-1024 cm^{-1} manifest slight shifts upon loading metal oxides relative to that of the commercial HY-zeolite at around 1042 cm^{-1}[36]. This demonstrated that the HY-zeolite retained its faujasite structure after metal oxides loading [37]. Another band around 1600 cm^{-1} related to H_2O bending vibrations confirmed the hygroscopic behavior of the nanocatalyst [38]. Small intense peaks in the range 455-469 cm^{-1} are attributed to the Zn-O bending vibrations whereas Ag-O bending vibrations emerged at 525-569 cm^{-1}.

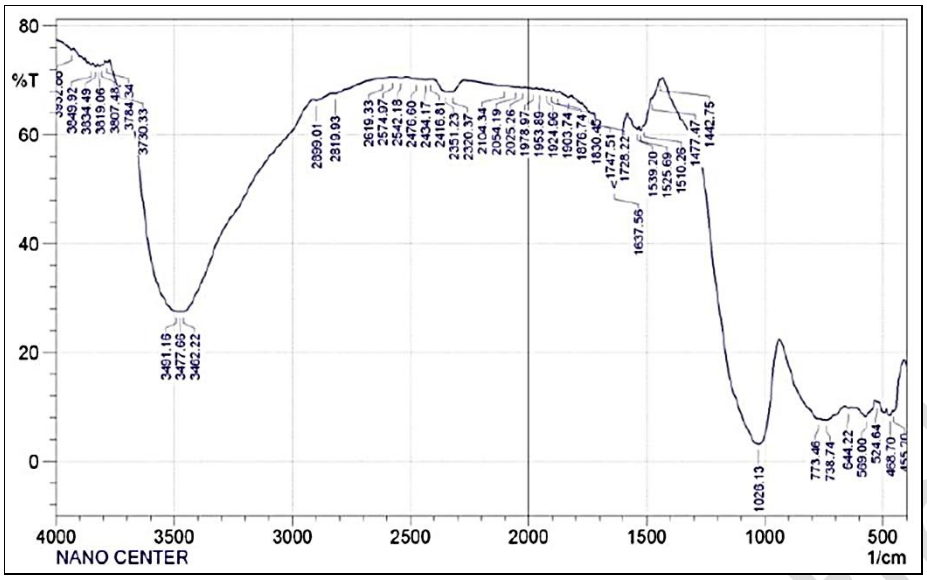

Figure 1. FTIR spectrum of the synthesized nanocatalyst

3.2 X-ray diffraction (XRD) studies

Fig. 2 shows the XRD patterns of our synthesized nanocatalyst, which displays the reflection planes (002), (111), (200), (202), (202) and (113) in the standard diffraction pattern of HY-zeolite (JCPDS Card No. 011-1829). The diffraction peaks at 35.45°, 39.84° and 43.36° well matched the standard diffraction pattern (JCPDS Card No. 01-1316) of ZnO nanoparticles. Peaks at 33.97°, 37.06°, 40.12°, 54.01° and 60-70° with reflection planes (111), (200), (220) and (311) well matched the standard diffraction pattern (JCPDS Card No. 74-1743) of AgO.

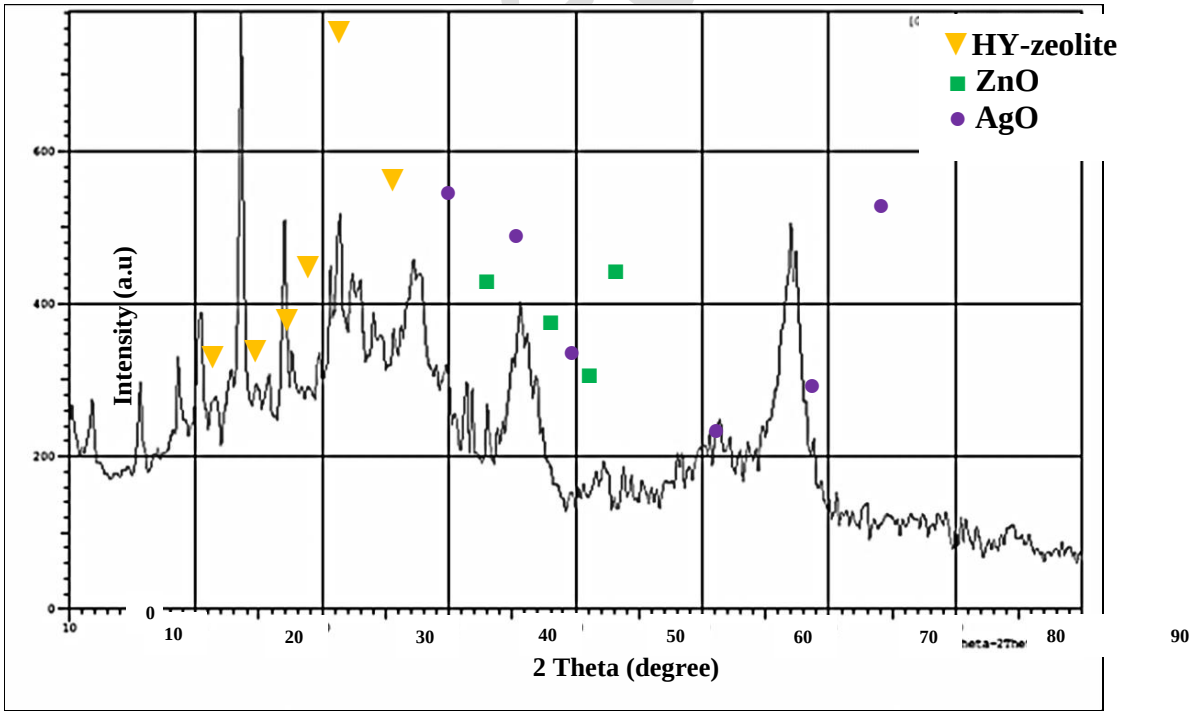

Figure 2. XRD pattern of the new synthesized nanocatalyst

3.3 BET analysis of the synthesized nanocatalyst

Brunauer-Emmett-Teller (BET) analysis was utilized to calculate the total surface area, pore volume and pore size of the newly synthesized AgO/ZnO/HY-zeolite nanocatalyst. The N_2 adsorption-desorption isotherms are illustrated in (Fig. 3 (a and b)). As shown in (Fig. 3 (a)), pristine HY-zeolite NPs manifested a microporous structure type IV isotherm (S_{BET}: 286 m^2g^{-1}) with strong N_2 uptake at relatively low P/P_0 demonstrating complete filling of the micropores. The pristine HY-zeolite NPs exhibited a micropore volume of (0.18 cm^3g^{-1}) and micropore size of (2.35 °A), whereas the prepared AgO:ZnO:HY-zeolite nanocatalyst showed a type IV isotherm with slight hysteresis loop indicating mesoporous moieties (Fig. 3 (b)). However, upon HY-zeolite impregnation by (2.5% wt) AgO and ZnO oxides, the S_{BET} and micropore size of the nanocatalyst implied a reduction from 286 m^2g^{-1} to 252 m^2g^{-1} and from 2.35°A to 2.15°A, respectively. In contrast, the micropore volume increased from 0.18 cm^3g^{-1} to 0.221 cm^3g^{-1}. These results may be caused by pore destruction after metal particles impregnation. Nonetheless, inclusion of metal oxide in the support framework leads to an increase in micropore volume [39].

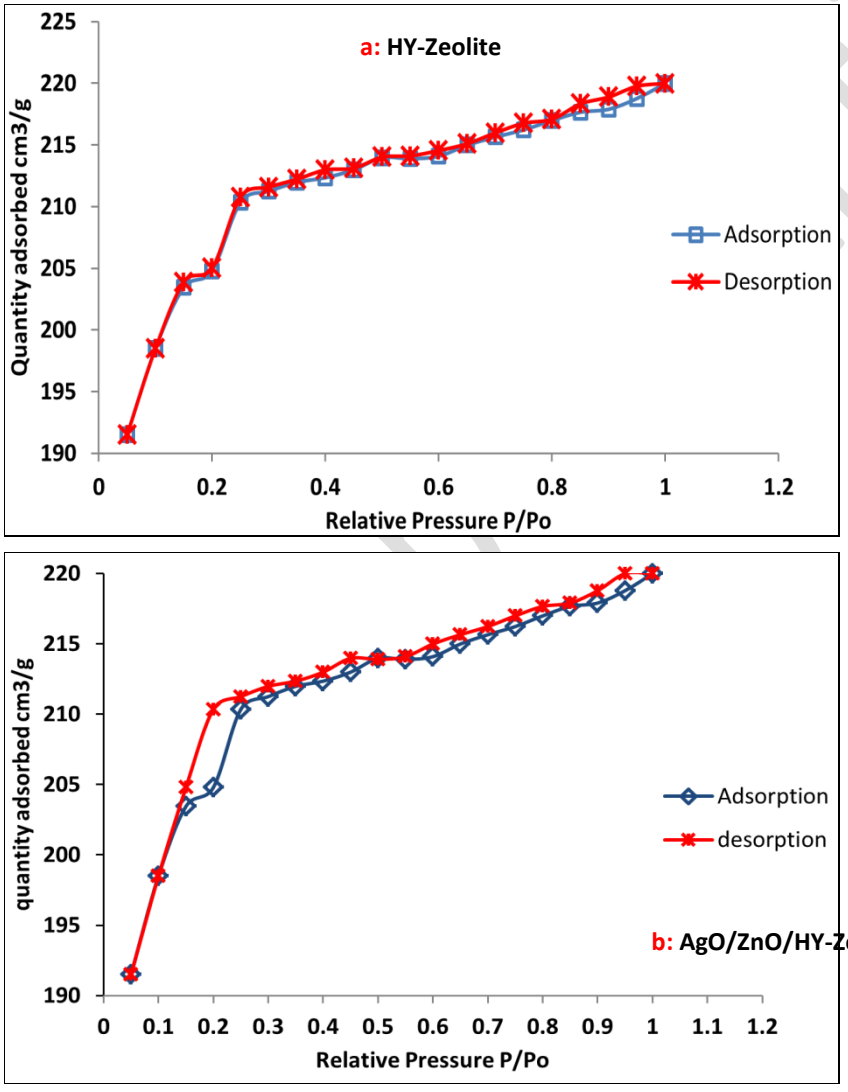

Figure 3. N_2 adsorption-desorption isotherms of (a) HY-zeolite thermally treated at 250°C and (b) newly synthesized nanocatalyst calcined at 600°C.

3.4 Surface morphology of the synthesized nanocatalyst

SEM was utilized to investigate the morphology, shape and size of the newly synthesized nanocatalyst with different magnifications as shown in (Fig. 4 (a-c)). Apparent well-distinguished agglomerates of nanocrystals with average particle size in the range 120-166 nm as well as some cavities are revealed for the pristine HY-zeolite NPs (Fig. 4 (a)). This type of morphology has previously been reported for HY-zeolite [30]. Irregularly ordered nano-textures under 1µm magnification (Fig. 4 (b)) with average particle size in the range 28-88 nm have been observed for the synthesized AgO/ZnO/HY-zeolite nanocatalyst. At higher magnification, sphere-like nano-textures belonging to the ZnO and AgO oxides were observed (Fig. 4 (c and d)). Furthermore, SEM images demonstrated that the morphology of the HY-zeolite NPs was preserved even after impregnation with 2.5% wt AgO and ZnO oxides.

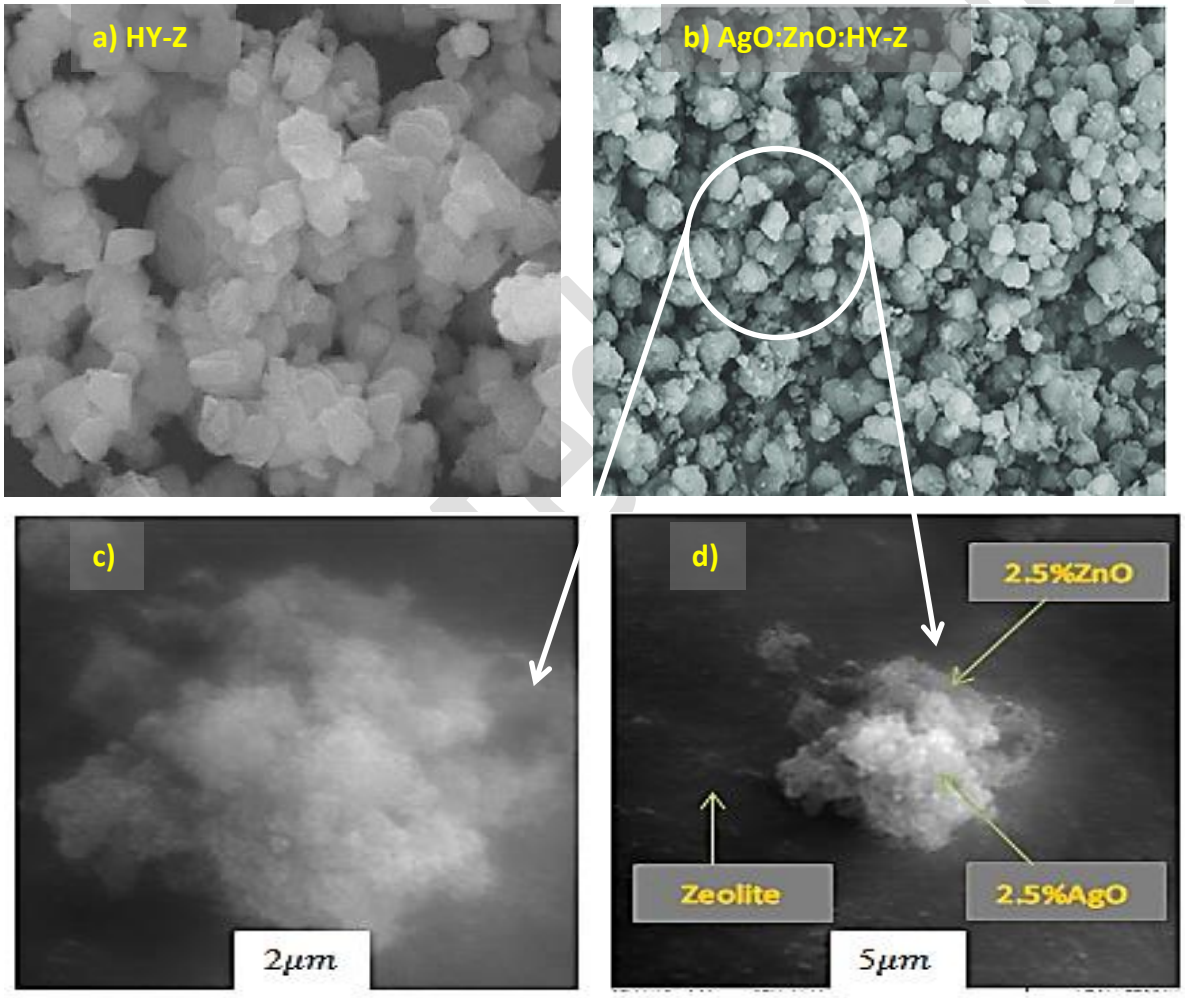

Figure 4. SEM images of (a) HY-zeolite after heat treatment above 250°C, (b) AgO/ZnO/HY-zeolite nanocatalyst at 1µm scale after calcination at 600°C, (c, d) AgO/ZnO/HY-zeolite nanocatalyst at 2µm and 5µm scale, respectively.

3.5 Optimizing of Cat-ODS operating conditions

In order to investigate the catalytic performance of our newly synthesized nanocatalyst, batch ODS reactions were carried out following previously published methodologies [20, 26, 40]. The operating variables such as reaction temperature, reaction time, catalyst dose and oxidant flowrate were carefully optimized for safe conditions and sulfur removal efficiency. The model light gasoil as

feedstock (150 ml at each run, S3 in supporting information) with 1200 ppm sulfur content (as DBT) was charged into the reaction vessel, heated to the desired temperature, mixed with previously-heated catalyst, and eventually oxidative desulfurization reaction occurred by air passing through the reaction medium. Thereafter, the reaction products (LGO and oxidized DBT molecules) were separated by extraction for 30 min with the appropriate solvent, followed by phase separation. The extracted light gasoil was then tested for sulfur content by energy-dispersive x-ray analysis. Literature works reported that including ZnO within nanocatalyst matrix has a positive effect on sulfur removal from a thermodynamic perspective [41, 42]. Moreover, it is noticed that the adsorption of organic sulfur compounds such as DBT on zinc oxide was spontaneous in nature. In addition, zinc oxide has a high equilibrium constant, high binding energy and fast oxidation kinetics which accelerate the oxidative reaction and achieve high sulfur removal efficiency. On the other hand, it is reported that incorporation of silver oxide into ODS catalyst matrix may combine the selective adsorption capacity of silver ions for sulfur compounds with the catalytic activity of ZnO/HY-zeolite which is helpful to enhance the selective oxidative desulfurization of diesel fuel [43]. This efficient selectivity for DBT molecules may attributed to good π-complexation between DBT and silver ions. Furthermore, using air as oxidant generates hydroperoxides *in situ*, thus enhancing the efficient oxidation of adsorbed DBT to their corresponding sulfoxides DBTO and sulfones $DBTO_2$ (S4 in supporting information) [44]. Since the adsorption of oxidized DBT products at the catalyst's active sites is reversible due to weak interactions among them, these polar products will be desorbed quite easily from the active sites.

3.6 Optimizing reaction temperature

Reaction temperature has a significant impact on the catalyst performance thus, it is very essential not to be neglected in the Cat-ODS process. Therefore, the temperature effect on the conversion of DBT in the current Cat-ODS process was examined by running a series of ODS experiments at different reaction temperatures (115, 135, and 165°C), different catalyst doses (0.4, 0.9, and 1.4g), with a constant reaction time of 60 min. As shown in (Fig. 5 and (S5) in supporting information), a distinct improvement in the DBT conversion from 49.1 % to 63.8 % at 0.4g, from 66.9% to 77.4% at 0.9g, and from 79.7% to 91.8% at 1.4g catalyst dose was observed upon temperature increase from 115°C to 165°C at constant air-flow rate. This valuable improvement in the conversion of DBT molecules with temperature increase may be attributed to overcoming the activation energy of the oxidation reaction. On the other hand, some previously published research reported that increasing the ODS reaction temperature would result in greater adsorption of oxidant and higher diffusion rate of DBT inside the catalyst pores where the oxidation reaction takes place, favouring higher conversion as a consequence [45, 46].

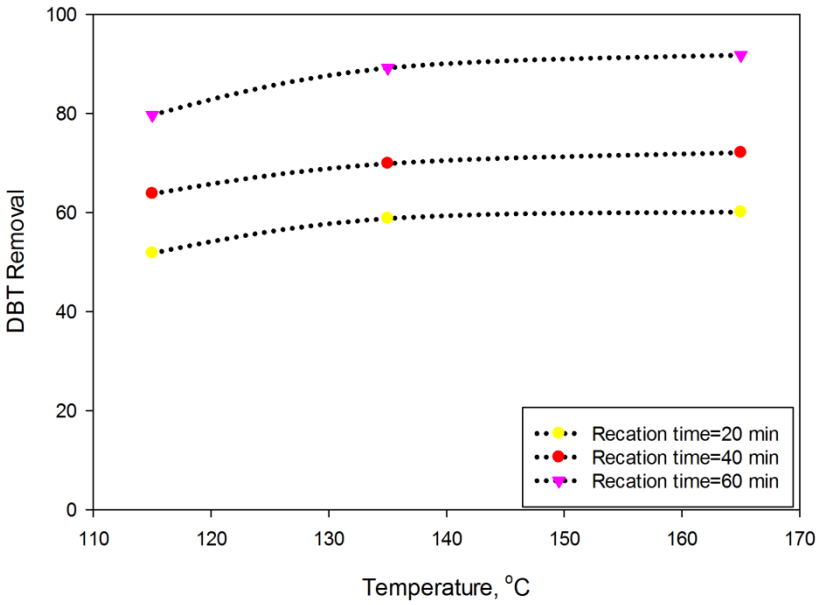

Figure 5. Effect of reaction temperature on the DBT conversion in the studied model LGO at different reaction time and 1.4g catalyst dose.

3.7 Optimizing reaction time

Determining the time required for the Cat-ODS reaction to complete is very important, firstly to prevent wasting energy or oxidizing LGO itself if time is too long and secondly, to ensure that there is enough time for the DBT conversion. Hence the effect of reaction time on the conversion of DBT by Cat-ODS has been optimized. Three time intervals (20, 40, and 60 min) were considered in batch Cat-ODS of the model light gasoil. As seen in (Fig. 6 and (S6) in supporting information), significant improvement in the conversion of DBT in the studied model LGO was observed with increasing reaction time. The maximum DBT conversion i.e. 63.8 % at 0.4g, 77.4% at 0.9g, and 91.8% at 1.4g catalyst dose was obtained at 60 min and 165°C reaction temperature. However, DBT conversion was still remarkable even after 60 min. Based on the previous studies of the catalytic activity in ODS processes, one can link this steady improvement in DBT conversion as time proceeds, to the need for sufficient interactions between DBT molecules and oxidant at the catalyst surface [47-49].

3.8 Optimizing catalyst dosage

The amount of catalyst used in the process of Cat-ODS is an economically important factor that has a direct effect on the process efficiency. However, (Fig. 7 and (S7) in supporting information) reveal the effects of catalyst dosage on the DBT conversion in the studied model light gasoil at different reaction temperatures and reaction times. A previous report shows that HY-zeolite without loaded metal oxides can achieve about 68% sulfur removal at 90 min, 60°C, and 8g of HY-zeolite per liter of fuel with 1000 ppm DBT [15]. In the present work, the DBT conversion increased strongly from 63.8% to 77.4% and finally 91.8% using 0.4, 0.9 and 1.4 g respectively of the AgO/ZnO/HY-zeolite nanocatalyst at 60 min and 165 ºC. The presence of metal oxides is therefore essential for deep oxidative desulfurization of diesel fuel. Nonetheless, the obtained results may be interpreted as follows: increasing catalyst dose will provide high surface area giving higher sulfur conversion. Such a high surface area may contributes in providing more active sites ready for oxidative reactions, as a result, the chances of DBT molecules interactions will increase and conversion rate increased.

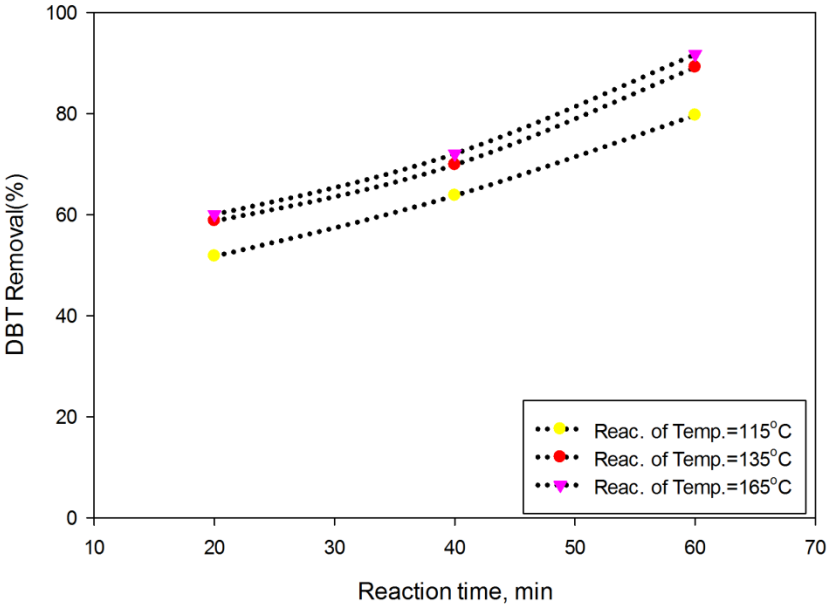

Figure 6. Effect of reaction time on the DBT conversion in the studied model LGO at different temperature and 1.4g catalyst dose.

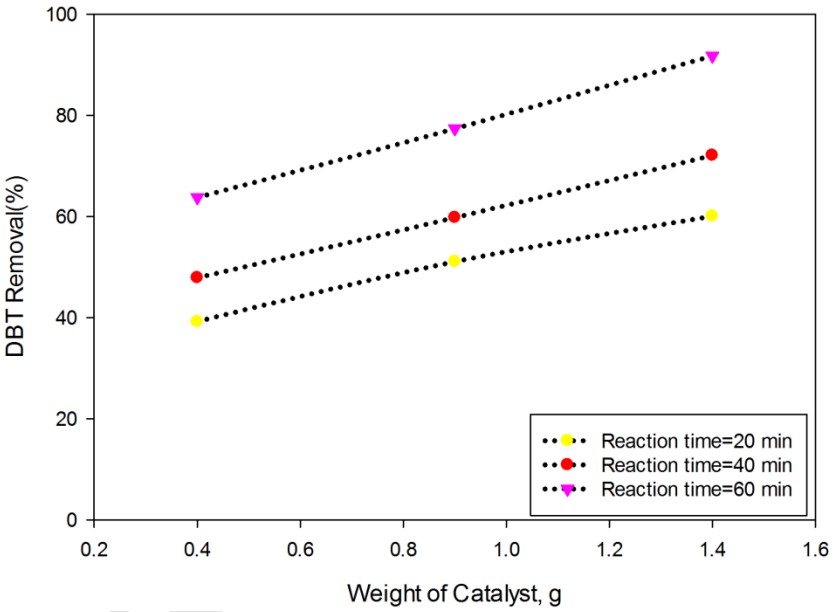

Figure 7. Effect of catalyst dosage on the DBT conversion in the studied model LGO at 160°C reaction temperature and different reaction times.

3.9 The reusability of the synthesized nanocatalyst

In general, the useable lifetime of the catalyst is an essential factor from the technological point of view. Herein, our new synthesized nanocatalyst used in ODS of the studied model LGO has been reused under the optimal conditions determined in this work. Fig. 8 illustrates the first cycle of the ODS reaction and the reusability of the nanocatalyst in the subsequent ODS runs at optimum conditions. The obtained results demonstrated that DBT conversion decreased from 91.8% to 86.650% after five cycles which indicates that the new synthesized nanocomposite is a promising nanocatalyst for catalytic oxidative desulfurization of DBT. The observed decline in the DBT

conversion may be attributable to poisoning of the catalyst surface by some water and/or sulfone adsorbed products.

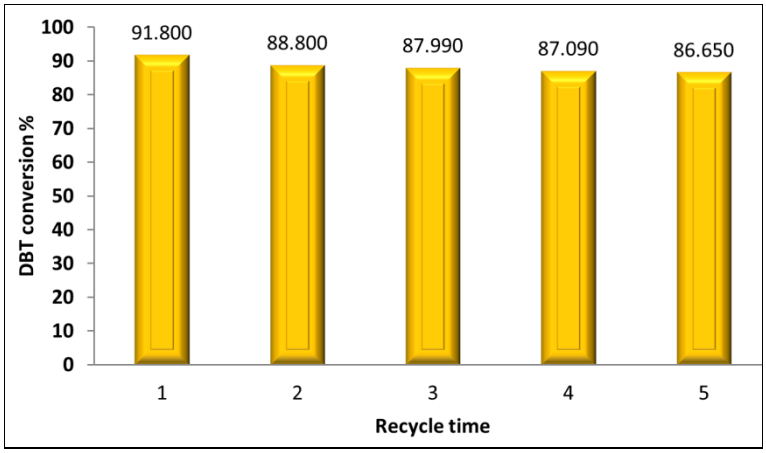

Figure 8. Reuseability of the AgO/ZnO/HY-zeolite nanocatalyst for the ODS of model light gasoil in this work.

4 Conclusion

A novel AgO/ZnO/HY-zeolite bimetallic nanocatalyst with equal amounts of metal oxides (2.5% wt of AgO and ZnO) has been successfully synthesized by a simple, low-cost impregnation method. The SEM and BET analysis for the synthesized nanocatalyst displayed irregularly ordered nano-textures with average particle size in the range 28-88 nm and surface area of 252 m^2g^{-1}. Surprisingly, screening catalytic performance during the ODS reactions demonstrated that our nanocatalyst had efficiently reduced the level of DBT (1200 ppm) in the model light gasoil with DBT conversion reaching 91.8% at 160°C reaction temperature, 60 min reaction time and 1.4g catalyst dose. The bimetallic components embedded in the zeolite matrix dramatically improved the catalytic activity, probably through reducing the energy barriers required for efficient adsorption of DBT onto the catalyst surface by good π-complexation between DBT and the active centres and accelerating the oxidative reaction. The results also indicated a very good reusability of the synthesized nanocatalyst with conversion rate reached 86.65% after five cycles. Beside the bimetallic feature, HY-zeolite support utilized herein has acceptable structural properties as a three-dimensional large pore diameter matrix which could facilitate mass transfer and provide shape selectivity for the nanocatalyst, rendering it a good potential candidate for Cat-ODS processes.

Supporting Information

For this article can be found under [Link provided by Wiley].

Acknowledgments

The authors highly appreciate the support provided by the SEC Faculty, Kingston University London. Great thanks go to the Department of Petroleum and Gas Refining Engineering College of Petroleum Process Engineering, Tikrit University Iraq.

ORCID iD

Omer Yasin Thayee Al-Janabi https://orcid.org/0000-0001-5435-112X

Peter J. S. Foot https://orcid.org/0000-0002-2122-3129

Abbreviations

BET: Brunauer-Emmett-Teller

Cat-ODS: catalytic oxidative desulfurization

DBT: dibenzothiophene

DBTO: dibenzosulfoxide

$DBTO_2$: dibenzosulfone

FTIR: Fourier transform infrared

LGO: light gasoil

M.wt: molecular weight

M.Fw: molecular formula

NCs: Nanocomposites

SEM Scanning electron microscopy

Th: thiophene

XRD X-ray diffraction

References

[1] A. M. Kermani, A. Ahmadpour, T. R. Bastami, M. Ghahramaninezhad, *New J. Chem.* 2018, *42 (14)*, 12188-12197. DOI: https://doi.org/10.1039/C8NJ01735B

[2] A. T. Jarullah, S. K. Aldulaimi, B. A. Al-Tabbakh, I. M. Mujtaba, *Chem. Eng. Res. Design*. 2020, *160*, 405-416. DOI: https://doi.org/10.1016/j.cherd.2020.05.015

[3] S. Vedachalam, P.E. Boahene, A. K. Dalai, *Energy & Fuels*. 2020, *344 (12)*, 15299-15312. DOI: https://doi.org/10.1021/acs.energyfuels.0c01527.

[4] H. Wang, I. Jibrin, X. Zeng, Front. *Chem. Sci. Eng*. 2020, *14 (4)*, 546-560. DOI: https://doi.org/10.1007/s11705-019-1842-z

[5] A. T. Jarullah, G. S. Ahmed, B. A. Al-Tabbakh, I. M. Mujtaba, *Comp. Chem. Eng.* 2020, *140*, 106869. DOI: https://doi.org/10.1016/j.compchemeng.2020.106869.

[6] A. M. El Naggar, H. A. El Sayed, A. A. Salem, N. E. Abd El-Sattar, *Ind. Eng. Chem. Res*. 2020, *59 (16)*, 7277-7290. DOI: https://doi.org/10.1021/acs.iecr.9b06058

[7] Y. Gao, L. Cheng, R. Gao, G. Hu, J. Zhao, *J. Hazardous Mater*. 2020, *401*, 123267. DOI: https://doi.org/10.1016/j.jhazmat.2020.123267

[8] L. Kamel, M. Anbia, *Silicon*. 2020, *12 (6)*, 1325-1336. DOI: https://doi.org/10.1007/s12633-019-00227-0

[9] H. Zhao, G. A. Baker, Q. Zhang, *Fuel*. 2017, *189*, 334-339. DOI: **Fehler! Linkreferenz ungültig.**

[10] H. Taghiyar, B. Yadollahi, *Sci. Total Environ*. 2020, *708*, 134860. DOI: **Fehler! Linkreferenz ungültig.**

[11] M. A. Rezvani, M. Shaterian, Z. Shokri Aghbolagh, R. Babaei, *Environ. Progress & Sustain. Energy*. 2018, *37*, 1891-1900. DOI: https://doi.org/10.1002/ep.12863

[12] M. A. Rezvani, M. Shaterian, F. Akbarzadeh, S. Khandan, *Chem. Eng. J*. 2018, *333*, 537-544. DOI: https://doi.org/10.1016/j.cej.2017.09.184

[13] S. Subhan, A.U. Rahman, M. Yaseen, H. U. Rashid, M. Ishaq, M. Sahibzada, Z. Tong, *Fuel*. 2019, *237*, 793-805. DOI: https://doi.org/10.1016/j.fuel.2018.10.067

[14] A. T. Nawaf, A. T. Jarullah, L. T. Abdulateef, *Bull. Chem. Reac. Eng. Catal*. 2019, *14*, 79-92. DOI: https://doi.org/10.9767/bcrec.14.1.2507.79-92

[15] M. Dadashi, G. Mazloom, A. Akbari, & F. Banisharif, *Environ. Sci. Pollut. Res*. 2020, *27*, 30600-30614. DOI: https://doi.org/10.1007/s11356-020-09266-2

[16] B. Jiang, H. Yaung, L. Zhang, R. Zhang, Y. Sun, Y. Huang, *Chem. Eng. J*. 2016, *283*, 89-96. DOI: https://doi.org/10.1016/j.cej.2015.07.070

[17] M. Zhang, J. Liu, J. Yang, X. Chen, M. Wang, H. Li, W. Zhu, H. Li, *Inorg. Chem. Front*. 2019, *6*, 451-458. DOI: https://doi.org/10.1039/C8QI00987B

[18] M. Zhang, J. Liu, H. Li, Y. Wei, Y. Fu, W. Liao, L. Zhu, G. Chen, W. Zhu, H. Li, *Appl. Catal. B.* 2020, *271*, 118936. DOI: https://doi.org/10.1016/j.apcatb.2020.118936

[19] M. A. Betiha, A. M. Rabie, H. S. Ahmed, A. A. Abdelrahman, M. F. El-Shahat, *Egypt. J. Pet.* 2018, *27*, 715-730. DOI: https://doi.org/10.1016/j.ejpe.2017.10.006

[20] F. Banisharif, M. R. Dehghani, M. Capel-Sánchez, J. M. Campos-Martin, *Catal. Today*. 2019, *333*, 219-225. DOI: https://doi.org/10.1016/j.cattod.2018.07.009

[21] H. Wang, M. Tang, F. Shi, R. Ding, L. Wang, J. Wu, B. Lv, *ACS Appl. Mater. Interf*. 2020, *12*, 38140-38152. DOI: https://doi.org/10.1021/acsami.0c10118

[22] I. V. Babich, J. A. Moulijn, *Fuel*. 2003, *82*, 607-631. DOI: https://doi.org/10.1016/S0016-2361(02)00324-1

[23] F. S. Mjalli, O. U. Ahmed, T. Al-Wahaibi, Y. Al-Wahaibi, I.M. Al-Nashef, *Rev. Chem. Eng*. 2014, *30*, 337-378. DOI: https://doi.org/10.1515/revce-2014-0001

[24] X. Xiao, H. Zhong, C. Zheng, M. Lu, X. Zuo, J. Nan, *Chem. Eng. J*. 2016, *304*, 908-916. DOI: https://doi.org/10.1016/j.cej.2016.07.022

[25] L. Kang, H. Liu, H. He, C. Yang, *Fuel*. 2018, *234*, 1229-1237. DOI: **Fehler! Linkreferenz ungültig.**

[26] F. Banisharif, M. R. Dehghani, M. Capel-Sánchez, J. M. Campos-Martin, *Ind. Eng. Chem. Res*. 2017, *5614*, 3839-3852. DOI: https://doi.org/10.1021/acs.iecr.7b00089

[27] M. Shi, D. Zhang, X. Yu, Y. Li, X. Wang, W. Yang, *Fuel Process. Technol*. 2017, *160*, 136-142. DOI: https://doi.org/10.1016/j.fuproc.2017.02.038

[28] Y. Yang, S. Mandizadeh, H. Zhang, M. Salavati-Niasari, *Sep. Purific. Technol*. 2020, *256*, 117784. DOI: https://doi.org/10.1016/j.seppur.2020.117784

[29] M. I. de Mello, E. V. Sobrinho, V. L. da Silva, S. B. Pergher, *Molec. Catal*. 2020, *482*, 100495. DOI: https://doi.org/10.1016/j.mcat.2018.02.009

[30] J. Yu, Z. Zhu, Q. Ding, Y. Zhang, X. Wu, L. Sun, J. Du, *Catal. Today*. 2020, *339*, 105-112. DOI: https://doi.org/10.1016/j.cattod.2019.05.053

[31] M. A. Rezvani, M. Shaterian, Z. S. Aghbolagh, R. Babaei. *Environ. Progress & Sustainable Energy*. **2018,** *37*, 1891-1900. https://doi.org/10.1002/ep.12863

[32] M. A. Rezvani, M. Shaterian, Z. S. Aghbolagh, F. Akbarzadeh, *ChemistrySelect* 2019, *4*, 6370. https://doi.org/10.1002/slct.201900202

[33] M. A. Rezvani, , Z. Maleki, *Appl. Organometal. Chem*. **2019**, *33*.e4895. https://doi.org/10.1002/aoc.4895

[34] M. A. Rezvani, Z. S. Aghbolagh, H. H. Monfared, *Appl. Organometal. Chem*. **2018**; *32*.e4592. https://doi.org/10.1002/aoc.4592

[35] M. A. Rezvani, S. Khandan, N. Sabahi, H. Saeidian, *Chinese J. Chem. Eng*. **2019,** *27*, 2418-2426. https://doi.org/10.1016/j.cjche.2018.10.024

[36] J. Cheng, Z. Zhang, X. Zhang, J. Liu, J. Zhou, K. Cen, *Int. J. Hydrog. Energy*. 2019, *44*, 1650-1658. DOI: https://doi.org/10.1016/j.ijhydene.2018.11.110

[37] A. Kostyniuk, D. Key, M. Mdleleni, *J. Saudi Chem. Soc*. 2019, *23*, 612-626. DOI: https://doi.org/10.1016/j.jscs.2018.11.001

[38] A. Teimouri, M. Mahmoudsalehi, H. Salavati, *Int. J. Hydrog. Energy*. 2018, *43*, 14816-14833. DOI: https://doi.org/10.1016/j.ijhydene.2018.05.102

[39] L. Kong, J. Li, Z. Zhao, Q. Liu, Q. Sun, J. Liu, Y. Wei, *Appl. Catal A. Gen*. 2016, *510*, 84-97. DOI: https://doi.org/10.1016/j.apcata.2015.11.016

[40] A. Akbari, M. R. Omidkhah, J. Towfighi Darian, *Ultrason. Sonochem*. 2014, *21*, 692-705. DOI: https://doi.org/10.1016/j.ultsonch.2013.10.004

[41] R. Sadegh-Vaziri, M.U. Babler, *Appl. Sci*. 2019, *9*, 5316. DOI: https://doi.org/10.3390/app9245316

[42] Y. Boukoberine, B. Hamada, *Arab. J. Catal*. 2016, *9*, 5522-5527. DOI: https://doi.org/10.1016/j.arabjc.2011.06.018

[43] L. Wu, F. Ye, D. Lei, et al., *Pet. Sci*. 2018, *15*, 857-869. DOI: https://doi.org/10.1007/s12182-018-0264-8

[44] A. Imtiaz, A. Waqas, I. Muhammad, *Chin. J. Catal*. 2013, *34*, 1839-1847. DOI: https://doi.org/10.1016/S1872-2067(12)60668-8

[45] G. S. Ahmed, A. T. Jarullah, B. A. Al-Tabbakh, I. M. Mujtaba, *J. Cleaner Prod*. 2020, *257*, 120436. DOI: https://doi.org/10.1016/j.jclepro.2020.120436

[46] M. A. Rezvani, F. Omid, *Chem. Eng. J*. 2019, *369*, 775-783. DOI: https://doi.org/10.1016/j.cej.2019.03.135

[47] W. N. A. Wan Mokhtar, W. A. Wan Abu Bakar, R. Ali, et al., *Clean Technol. Environ. Polic*. 2015, *17*, 1487-1497. DOI: https://doi.org/10.1007/s10098-014-0873-x

[48] L. Hao, S. A. Stoian, L. R. Weddle, Q. Zhang, *Green Chem*. 2020, *22*, 6351-6356. DOI: https://doi.org/10.1039/D0GC01999B

[49] W. Jiang, K. Zhu, H. Li, L. Zhu, M. Hua, J. Xiao, H. Li, et al., *Chem. Eng. J*. 2020, 394, 124831. DOI: https://doi.org/10.1016/j.cej.2020.124831

Figures and Tables legends

Table 1: indicate the physical properties of the studied model light gasoil (LGO)

Figure 1: FTIR spectrum of the synthesized nanocatalyst

Figure 2: XRD pattern of the new synthesized nanocatalyst

Figure 3: N_2 adsorption-desorption isotherms of (a) HY-zeolite thermally treated at 250°C and (b) newly synthesized nanocatalyst calcined at 600°C.

Figure 4: SEM images of (a) HY-zeolite after heat treatment above 250°C, (b) AgO/ZnO/HY-zeolite nanocatalyst at 1µm scale after calcination at 600°C, (c, d) AgO/ZnO/HY-zeolite nanocatalyst at 2µm and 5µm scale, respectively.

Figure 5: Effect of reaction temperature on the DBT conversion in the studied model LGO at different reaction time and 1.4g catalyst dose.

Figure 6: Effect of reaction time on the DBT conversion in the studied model LGO at different temperature and 1.4g catalyst dose.

Figure 7: Effect of catalyst dosage on the DBT conversion in the studied model LGO at 160°C reaction temperature and different reaction times.

Figure 8: Reuseability of the AgO/ZnO/HY-zeolite nanocatalyst for the ODS of model light gasoil in this work.